
Article:
Guillotin, D, Austin, P, Begum, R et al. (2017) Drug-repositioning screens identify Triamterene as a selective drug for the treatment of DNA Mismatch Repair deficient cells. Clinical Cancer Research, 23 (11). pp. 2869-2879. ISSN: 1078-0432

https://doi.org/10.1158/1078-0432.CCR-16-1216

Drug-repositioning screens identify Triamterene as a selective drug for the treatment of DNA Mismatch Repair deficient cells

Delphine Guillotin[1], Philip Austin[1,4], Rumena Begum[1,4], Marta O Freitas[1], Ashirwad Merve[2], Tim Brend[3], Susan Short[3], Silvia Marino[2] & Sarah A Martin[1]*

[1]Centre for Molecular Oncology, Barts Cancer Institute, Queen Mary University of London, Charterhouse Square, London, EC1M 6BQ, UK

[2]Blizard Institute, Barts and the London School of Medicine and Dentistry, Queen Mary University of London, 4 Newark Street, London, E1 2AT, UK

[3]Leeds Institute of Cancer and Pathology, Wellcome Trust Brenner Building St James's University Hospital, Beckett St, Leeds, LS9 7TF, UK

[4]Authors contributed equally to this work

[*]Corresponding Author: Sarah A. Martin

Centre for Molecular Oncology, Barts Cancer Institute, Queen Mary University of London, Charterhouse Square, London, EC1M 6BQ, UK

Email: sarah.martin@qmul.ac.uk

Tel: +44 (0)20 7882 3599

Fax: +44 (0)20 7882 3884

Conflict of Interest: The authors declare no conflicts of interest exist.

Running title: Triamterene selectively targets MMR-deficient cells

Statement of translational relevance

Loss of the DNA mismatch repair (MMR) pathway is a common feature of many tumor types. Due to the role of MMR proteins in the recognition of many drug-induced DNA adducts, MMR-deficient tumors are often resistant to a large number of currently used chemotherapies. Therefore, new selective therapies are urgently required for these patients. This manuscript reports the identification of a novel therapeutic strategy for the treatment of MMR-deficient tumors. We have shown that treatment with the diuretic drug Triamterene sensitizes MMR-deficient tumors *in vitro* and *in vivo*. This selectivity is through a Triamterene-mediated antifolate activity, dependent on thymidylate synthase expression. Given the frequency of MMR defects in a range of different tumor types, the implication of our work is that Triamterene may be used therapeutically to exploit this sensitivity in the clinic.

Abstract

Purpose: The DNA Mismatch repair (MMR) pathway is required for the maintenance of genome stability. Unsurprisingly, mutations in MMR genes occur in a wide range of different cancers. Studies thus far have largely focused on specific tumor types or MMR mutations, however it is becoming increasingly clear that a therapy targeting MMR-deficiency in general would be clinically very beneficial.

Experimental Design: Based on a drug-repositioning approach, we screened a large panel of cell lines with various MMR deficiencies from a range of different tumor types with a compound drug library of previously approved drugs. We have identified the potassium-sparing diuretic drug Triamterene, as a novel sensitizing agent in MMR-deficient tumor cells, *in vitro* and *in vivo*.

Results: The selective tumor cell cytotoxicity of Triamterene occurs through its antifolate activity, and depends on the activity of the folate synthesis enzyme, thymidylate synthase. Triamterene leads to a thymidylate synthase-dependent differential increase in reactive oxygen species in MMR-deficient cells, ultimately resulting in an increase in DNA double strand breaks.

Conclusion: Conclusively, our data reveal a new drug repurposing and novel therapeutic strategy that has potential for the treatment of MMR-deficiency in a range of different tumor types and could significantly improve patient survival.

Introduction

Germline mutations in DNA mismatch repair (MMR) genes, including MLH1, MSH2, MSH6 and PMS2 can lead to Lynch Syndrome, an autosomal condition also known as hereditary non polyposis colorectal cancer (HNPCC)(*1*). Patients with this condition have an 80% lifetime risk of developing colorectal cancer and a 60% lifetime risk of developing endometrial cancer. In addition, patients are also at an increased risk of developing other cancers such as small bowel, pancreatic, prostate, urinary tract, liver, kidney, and bile duct cancer. Defects in the MMR system can also occur as a result of somatic mutations or epigenetic silencing. Significantly, it is thought that 15% of all colorectal cancers and 30% of all endometrial cancers have loss of a functional MMR pathway (*2, 3*). Furthermore, mutations in the MMR gene, MSH6 have been identified in 26-41% of temozolomide-resistant glioblastoma (GBM) patients and mediate temozolomide resistance (*4-6*). More recently, a number of studies have shown that a reduction in MMR protein levels, in particular MSH2 and MSH6, occurs upon GBM recurrence and that transcript levels of MMR genes are prognostic for patient survival after temozolomide treatment (*6-8*).

Synthetic lethality with loss of DNA repair proteins has previously been successfully exploited (*9-13*). To date, a number of studies have identified synthetic lethal interactions with specific MMR gene mutations or specific tumor types (*9, 10, 14, 15*). In this study, we carried out drug-repositioning compound screens in a panel of MMR-deficient cellular models from a range of different tumor types, to identify drugs that sensitize with MMR loss in general. We identified the potassium-sparing diuretic drug, Triamterene as a novel therapeutic agent in MMR-deficient tumor cells. Our data suggest that the selectivity of Triamterene is based on its anti-folate activity and is dependent on expression of the folate synthesis enzyme, thymidylate synthase. Taken together, our

data reveals that Triamterene is a promising novel therapeutic strategy for the treatment of MMR-deficient disease in a range of different tumor types.

Materials and Methods

Cell lines

The U251.TR3 GBM cell lines were a kind gift from Dr. David Louis (Massachusetts General Hospital, MA, USA). In the original paper (*5*), the nomenclature for these cell lines was A172.TR3. In a subsequent correction to the paper, this nomenclature was updated to U251.TR3 (MSH6-) (*16*). We have STR profiled these cell lines and confirm they originate from U251 cells. The U251 (MMR+), MFE-280 (MMR+), MFE-296 (MLH1-), KLE (MMR+), AN3CA (MLH1-), HEC1B (MSH6-), RL95-2 (MSH2-, MSH6-, MSH3-) and ISHIKAWA (MLH1-) cell lines were purchased from ATCC. The colorectal DLD1 (MSH6-) and DLD1+Chr2 (MMR+) cell lines and endometrial HEC59 (MSH2-) cell lines were a kind gift from Dr. Thomas Kunkel (National Institute of Environmental Health Sciences). The human colon cancer cell line HCT116 (MLH1-) and HCT116+Chr3 (MMR+) were a kind gift from Dr. Alan Clark (NIEHS). DLD1 and DLD1+Chr2 cells were grown in RPMI (Sigma-Aldrich), 10% FBS and 1% penicillin-streptomycin at 37 $^{\circ}$C with 5% CO_2. All other cell lines were grown in DMEM (Sigma-Aldrich), 10% FBS and 1% penicillin-streptomycin at 37 $^{\circ}$C with 5% CO_2. DLD1+Chr2 and HCT116+Chr3 cells were maintained under selective pressure of 400 μg/mL geneticin (G418 sulfate, Roche). U251.TR3 cells were maintained in 100 μM TMZ (Santa Cruz). All cell lines were authenticated on the basis of STR-profile, viability, morphologic inspection, and were routinely mycoplasma tested.

Compound Library Screen

The FDA-approved compound library incorporating 1120 drugs was purchased from Selleck Chemicals. Cells were plated in 96-well plates and treated with vehicle (0.01% DMSO) or the compound library (average compound concentration of the library in

media was 10 μM). After 4 days incubation with the drug library, cell viability was assessed using the CellTiter Glo assay (Promega) according to the manufacturer's instructions. Luminescence readings from each well were log transformed and normalized according to the median signal on each plate and then standardized by use of a Z-score statistic, using the median absolute deviation to estimate the variation in each screen. Z-scores were compared to identify compounds that cause selective loss of viability in MMR-deficient cells, in comparison to MMR-proficient cells. For validation experiments, cells were treated with increasing concentrations of Triamterene and cell viability using the CellTiter Glo assay was assayed after 5 days. Triamterene was purchased from Sigma-Aldrich. N-acetyl cysteine was purchased from Santa Cruz.

Colony formation assay

Validation of Triamterene was performed by colony formation assays. Cells were seeded at various densities in six-well plates and exposed to the drug at the indicated concentrations. Cells were retreated every four days, whereby the drug containing media was removed and the fresh drug containing media was added. After ten to fourteen days, cells were fixed and stained with sulphorhodamine-B (Sigma, St. Louis, USA) and counted.

Cell Cycle Analysis

Following Triamterene treatment, cells were fixed in 70% ice-cold ethanol and stained with 4% propidium iodide (PI) and 10% RNase A in PBS for cell-cycle analysis. The sample readout was performed on the BD LSRFortessa (Becton Dickinson, USA), and the data were analysed using FlowJo (FlowJo LLC).

Xenograft experiments

DLD1 and DLD1+Chr2 cell lines (1.6 x 10^6 cells) re-suspended in PBS, were injected subcutaneously into the right flank of adult (~10 weeks old) male NOD-SCID mice (Charles-River Laboratories). Tumors were allowed to develop to a mean tumor diameter between 4 and 8 mm before treatment. Mice were then treated 3 times a week by gavage, with 25 mg/kg Triamterene or vehicle. Tumors were measured twice weekly. Mice were sacrificed in case of sickness or when the tumors reached 1.44cm^2. All animal procedures were carried out as per the Animal Scientific Procedures Act 1986, under the Home Office approval licenses (PPL-70/7275 and PIL-70/23444).

Protein analysis

Cell pellets were lysed in 20 mM Tris (pH 8), 200 mM NaCl, 1 mM EDTA, 0.5% (v/v) NP40, 10% glycerol, supplemented with protease inhibitors. For western blotting, lysates were electrophoresed on Novex precast gels (Invitrogen) and immunoblotted using the following antibodies: anti-MSH6 (#5424), anti-MSH2 (#2017), anti-MLH1 (#4256), anti-thymidylate synthase (#9045), β-Actin (#4970), purchased from Cell Signaling. The following antibodies were also used; anti-MSH3 (sc-11441; Santa Cruz) and anti β-tubulin (T8328; Sigma). This was followed by incubation with anti-IgG-horseradish peroxidase and chemiluminescent detection (Supersignal West Pico Chemiluminescent Substrate, Pierce). Immunoblotting for β-Actin and β-tubulin were performed as loading control.

siRNA transfections

For siRNA transfections, cells were transfected with individual siRNA oligos (Qiagen) using Lipofectamine RNAiMax (Invitrogen) according to the manufacturer's instructions.

As a control for each experiment, cells were left un-transfected or transfected with a non-targeting control siRNA and concurrently analyzed.

Reactive Oxygen Species Detection

Cellular ROS was measured using DCFDA-Cellular Reactive Oxygen Species Detection Assay Kit (Abcam, ab113851) according to the manufacturer's instructions. Briefly, to detect ROS levels, non-fluorescent 2',7'-dichlorofluorescein diacetate (DCFDA) is converted to fluorescent DCF upon ROS (H_2O_2, •OH, $ONOO^-$ and $•O_2^-$) induction. Cells were plated in clear bottom black 96-well plates and treated with Triamterene for the indicated times. Cells were then treated with 20 μM DCFDA or incubated in assay buffer as a negative control. After 30 min incubation at 37˚ C, cells were washed with 1X PBS and incubated for 4 h in fresh assay buffer at 37˚ C in a 5% CO_2 incubator. Fluorescence was measured, using the Wallac 1420 plate reader (PerkinElmer). Each assay condition was performed in duplicate and cell viability was measured in replicate plates using the CellTiter-Glo assay. Fluorescence DCF values were normalized to the corresponding cell viability luminescence data.

Detection of cellular DNA damage by Comet assay

A commercially available Comet assay kit from Cell Biolabs (STA-351) was used to measure levels of cellular DNA damage. The assays were performed according to the manufacturer's instructions. Briefly, 1 x 10^5 cells were mixed with molten agarose. DNA from embedded cells was then denatured in an alkaline solution. Samples were electrophoresed in a horizontal chamber to separate intact DNA from damaged fragments. Following electrophoresis, samples were then stained with a Vista Green DNA dye, and visualized by fluorescence microscopy. Cellular DNA damage is

visualised as it migrates further than intact DNA and results in a comet tail shape. For assessment of the Comet assay, 50 comets were scored per condition and ImageJ was used to quantify the intensity and score the comets using the following calculation: Tail DNA % = 100 X Tail DNA Intensity/Cell DNA intensity.

Estimation of 8-oxodG levels

A commercially available ELISA kit from Cell Biolabs (STA-320) was used to measure levels of 8□oxodG. Although this 8-oxodG ELISA has potential shortcomings for the precise quantification of 8-oxodG levels, it allows an estimation of the change of 8-oxodG levels upon triamterene treatment. Genomic DNA was extracted using the QIamp DNA isolation kit (Qiagen), digested with nuclease P1, treated with calf intestinal phosphatase and denatured. To avoid artifactual production of 8-oxodG, we used a phenol-free method of DNA isolation and DNA was completely digested. The assays were performed according to the manufacturer's instructions. Briefly, 10-15 µg DNA from untreated and treated cells or the 8□oxodG standard (0.078–20 ng/ml) was incubated with an 8□oxodG monoclonal antibody in an 8□oxodG-precoated microtiter plate. The assay was normalized by using an equal amount of DNA for each sample. Standard curves were calculated with serial dilutions of 8□oxodG standard to calculate reaction efficiency. Samples were assayed in triplicate.

Detection of γH2AX Foci by immunofluorescence

Cells were seeded onto poly-lysine coated coverslips and treated with drugs as indicated. After 48 hrs treatment, cells were fixed for 10 min with 4% PFA in PBS. Cells were then permeabilized with Triton, blocked for 1 h at room temperature and subsequently incubated with γH2AX antibody (#05-636, Millipore) for 18 h at 4 °C. This

was followed by incubation with anti-IgG-Alexa568 (#A11031, Invitrogen). Coverslips were then washed in 4% DAPI/1X PBS and mounted with ProLong® gold antifade mounting solution (Invitrogen). Slides were imaged using a Zeiss LSM 510 confocal microscope. Per condition, a minimum of 300 cells were counted and quantified for γH2AX positive cells (> 5 foci per nucleus).

Statistical analysis

Unless otherwise stated, data represent standard error of the mean of at least three independent experiments. The two-tailed paired Student's t test was used to determine statistical significant with $p<0.05$ regarded as significant. For confocal experiments, images are representative of at least three independent experiments, where a minimum of 300 cells were analyzed.

Results

MMR deficiency increases the toxicity of triamterene in a range of tumor-derived cell lines

To identify compounds that can sensitize MMR-deficient cells, we screened a large panel of cell lines with a range of different MMR gene mutations from a number of tumor types. These included the MSH6-deficient colorectal cancer cell line DLD1 and its isogenic MSH6-proficient DLD1+Chr2 cell line (Figure 1A), the previously characterized temozolomide-resistant MSH6-deficient U251.TR3 GBM cell line and the isogenic MSH6-proficient U251 cell line (Figure 1B; (*5, 16*)) and a panel of endometrial cancer cell lines; KLE (MMR-proficient), MFE-280 (MMR-proficient), MFE-296 (MLH1-deficient), ISHIKAWA (MLH1-deficient) and HEC1B (MSH6-deficient; Figure 1C).

Based on the concept of drug repositioning, of identifying previously approved compounds for new clinical indications, cells were screened in the presence of either vehicle (DMSO) or a compound library comprising 1018 FDA-approved drugs. This approach aimed to identify compounds with previous unknown potential for repurposing as MMR-selective drugs. Analysis of our screens revealed that the potassium-sparing diuretic compound, Triamterene was a promising candidate for a new MMR-selective drug. Validation experiments revealed that, although the sensitization was variable depending on the MMR-defect, however when compared to the MMR-proficient cells, treatment with Triamterene induced toxicity over a range of concentrations specifically in MMR-deficient cells (Figure 1D-F). Triamterene also caused sensitivity in MMR-deficient cells, in comparison to MMR-proficient cells, in a clonogenic survival assay (Figure 1G).

To further investigate this selectivity for MMR deficiency, we measured cell viability of the MLH1-deficient colorectal cancer cell line HCT116 and its isogenic matched-paired MLH1-proficient cell line, HCT116+Chr3 when treated with Triamterene (Figure 1H). Significantly, Triamterene also induced selectivity in the MLH1-deficient HCT116 cells, but not in MLH1-proficient cells. Significantly, we observed selectivity in all MMR deficient cell lines tested, regardless of MMR mutation or tumor type, while no significant effect was observed in MMR-proficient cells. This suggests that Triamterene is selective with loss of MMR pathway function and may provide a novel therapeutic strategy in a wide range of cancers.

Triamterene cytotoxicity occurs through its antifolate activity and requires thymidylate synthase expression

Previous studies have shown that Triamterene can act as both an inhibitor of the epithelial sodium channel (ENaC) (*17*) and also as an antifolate (*18*). Therefore, to

determine the mechanism underlying the observed Triamterene-induced cytotoxicity with MMR-deficiency, we performed siRNA-mediated depletion of a panel of ENaC isoforms (α, β & γ) previously suggested to be inhibited by Triamterene and analyzed cell viability (Figure 2A). We observed no differential cytotoxicity upon targeting the ENaC isoforms, either alone or in combination, which suggests that the observed selectivity is not due to ENaC inhibition. We next determined whether Triamterene-mediated selectivity was due to its anti-folate activity. To this end, we measured the cell viability of MMR-deficient and proficient cells treated with folates (dihydrofolate and tetrahydrofolate) in addition to Triamterene. We observed that the selectivity of Triamterene for MMR deficiency could be rescued by the addition of folates (Figure 2B & 2C), therefore suggesting that Triamterene is selective through its anti-folate activity.

To further analyze the anti-folate effect of Triamterene, we analyzed the requirement for thymidylate synthase in Triamterene-mediated selectivity. Thymidylate synthase is the only *de novo* enzyme for dTMP synthesis. It catalyzes the reductive transfer of a methyl group from N^5,N^{10}-methylenetetrahydrofolate (CH_2-THF) to dUMP, forming dTMP and dihydrofolate (DHF). Our results suggest that thymidylate synthase protein expression is not altered upon Triamterene treatment (Figure 2D). However, silencing thymidylate synthase by siRNA prevents Triamterene-induced lethality in MMR-deficient cells (Figure 2E & 2F; Supplementary Figure 1A). These results suggest that thymidylate synthase expression is necessary for the Triamterene-mediated selectivity in MMR-deficient cells. Furthermore, treatment with the clinically approved thymidylate synthase inhibitors, 5-FU and Raltitrexed, also rescued the Triamterene-induced cytotoxicity in MMR-deficient cells (Supplementary Figure 1B). Taken together, our results suggest that Triamterene-induced selectivity is due to the anti-folate activity of Triamterene and is dependent on thymidylate synthase expression.

Triamterene-induced cytotoxicity depends on increased ROS levels

It has previously been shown that folate starvation can increase ROS levels, leading to cellular oxidative stress (*19*). Our previous studies have shown that an increase in oxidative stress is synthetically lethal with MMR deficiency (*9, 10, 14, 15*). Therefore, we investigated whether Triamterene can induce an increase in ROS levels due to folate inhibition in MMR-deficient and -proficient cells. To this end, we treated MMR-deficient and -proficient cells with increasing concentrations of Triamterene and measured ROS levels (Figure 3A & B). Our results show a greater increase in the level of ROS in Triamterene-treated MMR-deficient cells, in comparison to MMR-proficient cells. To further investigate if this increase in ROS levels in MMR-deficient cells was responsible for Triamterene selectivity, we treated cells with Triamterene alone or in combination with the ROS scavenger, N-acetylcysteine (NAC; Figure 3C). Our results demonstrate that the Triamterene-induced selectivity in MMR-deficient cells can be rescued by addition of NAC, which suggests that increased ROS levels are, at least in part, the mechanism of toxicity upon Triamterene treatment. Our data indicates the importance of thymidylate synthase expression in triamterene-induced selectivity. To further investigate this, we analyzed ROS levels upon thymidylate synthase silencing and Triamterene treatment (Figure 3D & E). Interestingly, we observed that silencing thymidylate synthase by siRNA prevents the Triamterene-induced increase in ROS levels. These results suggest that thymidylate synthase is required for ROS accumulation, leading to Triamterene cytotoxicity.

Our results suggest that MMR-deficient cells have reduced cellular viability upon Triamterene treatment. To investigate the mechanism of this selectivity further, we stained cells, before and after Triamterene treatment, with propidium iodide and

measured cells by flow cytometry to determine which phase of the cell cycle they accumulated in after treatment (Figure 4A). Interestingly, our results suggest that upon Triamterene treatment, MMR-deficient cells arrest in the G2/M phase of the cell cycle, corresponding to the reduced cellular viability we observed. An increase in ROS levels can lead to cellular DNA damage, including DNA single-strand breaks, alkali-labile sites, oxidative DNA damage and ultimately an increase in DNA double strand breaks (DSB), thereby triggering cell cycle arrest. To assess if Triamterene induces DNA damage in MMR-deficient cells, we measured cellular DNA damage including DNA fragmentation and DNA strand breaks using the comet assay (Figure 4B). Treatment with Triamterene resulted in an increase in DNA damage in the MMR-deficient cells only. To further investigate the type of DNA damage induced, we measured accumulation of the oxidative DNA lesion, 8-Oxo-2'-deoxyguanosine (8□oxodG) using an ELISA assay (Figure 4C). We observed a significant increase in 8□oxodG DNA lesions in the Triamterene-treated MMR-deficient cells only. To determine whether this oxidatively damaged DNA, resulted in DNA double strand breaks triggering cell cycle arrest, we measured γH2AX foci, a marker for DNA DSBs, by confocal microscopy (Figure 5A-D). Treatment with Triamterene induced an increase in γH2AX foci in MMR-deficient cells, which can be rescued by addition of the ROS scavenger, NAC. Taken together, our results suggest that Triamterene treatment leads to an increase in ROS levels in MMR-deficient cells, which ultimately leads to an increase in 8-oxodG DNA lesions and DNA DSBs, resulting in cell cycle arrest (Figure 4D).

Triamterene can re-sensitize MMR-deficient cells *in vivo*

To examine the *in vivo* efficacy of Triamterene, the MMR-deficient and MMR-proficient DLD1 and DLD1+Chr2, respectively, colorectal cancer cells, were injected subcutaneously into NOD-SCID mice. Xenografted mice were subjected to treatment 3

times a week with Triamterene or vehicle (PBS). We observed that tumor growth from the MMR-deficient xenografts was significantly reduced (p=0.01) by Triamterene treatment when compared to vehicle (Figure 6A). In addition, no difference in tumor growth was observed in the Triamterene treated MMR-proficient xenograft tumors when compared to vehicle, further validating Triamterene as a compound that specifically targets cancer cells with deficient MMR pathways (Figure 6B). Taken together, these *in vivo* observations further indicate that Triamterene treatment has potential clinical utility in patients with MMR-deficient, for which therapeutic options are scarce.

DISCUSSION

Through a compound screen, we identified the diuretic drug Triamterene as an *in vitro* and *in vivo* selective compound with MMR deficiency. Collectively, our data argues that stratifying patients according to their MMR status would prove efficacious with regards to treatment with Triamterene. Furthermore, our data suggests that levels of thymidylate synthase govern sensitivity to Triamterene in MMR-deficient cells. Upon thymidylate synthase inhibition, treatment with Triamterene was no longer selective suggesting that thymidylate synthase levels determine the balance between Triamterene resistance and sensitivity in these cells. Our data suggest that folate inhibition and thymidylate synthase are critical for the triamterene selectivity in MMR-deficient cells, however we cannot exclude the fact that other pathways may also be influencing this effect, at least in part. One of the most intriguing findings from this work is the requirement for thymidylate synthase for the induction of ROS upon Triamterene treatment. It is likely due to an activity of thymidylate synthase in the absence of sufficient levels of methyl donor CH2-THF, thus leading to ROS. It would be interesting to understand whether thymidylate synthase is regulating ROS levels through NAPDH oxidase complexes or providing protection against ROS production through the antioxidant response. Numerous studies

have investigated ROS induction upon treatment with thymidylate synthase inhibitors, but, to our knowledge, no study has identified a role for thymidylate synthase in the regulation of ROS levels. Previously, antifolate agents targeting the folate metabolic enzyme dihydrofolate reductase (DHFR), such as methotrexate and pemetrexed, were identified as cytotoxic in MSH2-deficient cells, but not in other MMR-deficient cell lines (*9, 20*). Perhaps this is due to the generation of specific DNA lesions upon DHFR inhibition in MSH2-deficient cells, rather than a more general inhibition of folate metabolism upon Triamterene treatment. Taken together, these data also suggest a potential difference in the folate metabolic pathway in MMR-deficient and -proficient cell lines.

An increase in ROS levels can lead to cellular DNA damage, including DNA fragmentation, oxidative DNA damage and ultimately an increase in DNA double strand breaks (DSB), thereby triggering cell cycle arrest. We observed a significant increase in cellular DNA damage, and more specifically 8-oxodG DNA lesions in the Triamterene-treated MMR-deficient cells only. Our data suggest that these lesions, if incompletely repaired, can induce DNA DSBs, which ultimately result in the cell cycle arrest and reduced cellular viability we observe.

We and others have focused largely on targeting loss of DNA repair in tumor cells. However, recent advances indicate that targeting both the tumor cell and its interaction with the immune microenvironment may significantly improve patient benefit. A recent Phase II clinical trial in patients with deficiency in the MMR pathway indicated that MMR status predicted clinical benefit with the PD-1 inhibitor pembrolizumab (*21*). However, only 50% of MMR-deficient patients responded to pembrolizumab, suggesting that selectively targeting MMR-deficient tumor cells with for example Triamterene, in

combination with immune checkpoint inhibitors may increase therapeutic efficacy and may prove to be more clinically beneficial.

In this study we exploit the concept of drug repurposing, which is the discovery of new indications for existing drugs, to identify novel selective drugs for the treatment of MMR-deficient tumors. Repositioning of drugs highlights an increasingly effective means of drug discovery. In addition to the reduced cost and time commonly associated with traditional drug discovery, the advantage of drug repositioning strategies is the fact that existing drugs have already been used in patients and, therefore, their toxicity and safety profiles are already established. Hence, drugs identified in drug repositioning approaches can enter clinical trials rapidly, thereby maximizing their potential benefit to patients. Here, we have shown for the first time that Triamterene, originally developed as a diuretic, has anti-tumor activity and we provide evidence of its efficacy in a range of MMR-deficient tumor types.

Grant support

This work was supported by funding from the Barts and The London Charity (467/1505), Wellbeing of Women charity (RG1629) and Cancer Research UK (C16420/A18066).

Acknowledgements

We thank Dr. D. Louis, Dr. T. Kunkel and Dr. A. Clarke for the provision of cell lines. We thank J. Andow-Cleaver, T. Chaplin-Perkins and H. Schmidt for their help with animal work. This research was supported by the BCI Flow Cytometry and Microscopy Facilities. We thank Dr. P. S. Ribeiro and Dr. T. V. Sharp for critical reading of the manuscript. We also thank all members of the Martin lab for helpful discussions.

REFERENCES

1. Lynch HT, Snyder CL, Shaw TG, Heinen CD, Hitchins MP. Milestones of Lynch syndrome: 1895-2015. *Nat Rev Cancer* 2015;**15**:181-94.
2. Imai K, Yamamoto H. Carcinogenesis and microsatellite instability: the interrelationship between genetics and epigenetics. *Carcinogenesis* 2008;**29**:673-80.
3. Resnick KE, Frankel WL, Morrison CD, Fowler JM, Copeland LJ, Stephens J, et al. Mismatch repair status and outcomes after adjuvant therapy in patients with surgically staged endometrial cancer. *Gynecol Oncol* 2010;**117**:234-8.
4. Cahill DP, Levine KK, Betensky RA, Codd PJ, Romany CA, Reavie LB, et al. Loss of the mismatch repair protein MSH6 in human glioblastomas is associated with tumor progression during temozolomide treatment. *Clin Cancer Res* 2007;**13**:2038-45.
5. Yip S, Miao J, Cahill DP, Iafrate AJ, Aldape K, Nutt CL, et al. MSH6 mutations arise in glioblastomas during temozolomide therapy and mediate temozolomide resistance. *Clin Cancer Res* 2009;**15**:4622-9.
6. Felsberg J, Thon N, Eigenbrod S, Hentschel B, Sabel MC, Westphal M, et al. Promoter methylation and expression of MGMT and the DNA mismatch repair genes MLH1, MSH2, MSH6 and PMS2 in paired primary and recurrent glioblastomas. *Int J Cancer* 2011;**129**:659-70.
7. McFaline-Figueroa JL, Braun CJ, Stanciu M, Nagel ZD, Mazzucato P, Sangaraju D, et al. Minor changes in expression of the mismatch repair protein MSH2 exert a major impact on glioblastoma response to temozolomide. *Cancer Res* 2015;**75**:3127-38.
8. Stark AM, Doukas A, Hugo HH, Hedderich J, Hattermann K, Maximilian Mehdorn H, et al. Expression of DNA mismatch repair proteins MLH1, MSH2, and MSH6 in recurrent glioblastoma. *Neurol Res* 2015;**37**:95-105.
9. Martin SA, McCarthy A, Barber LJ, Burgess DJ, Parry S, Lord CJ, et al. Methotrexate induces oxidative DNA damage and is selectively lethal to tumour cells with defects in the DNA mismatch repair gene MSH2. *EMBO Mol Med* 2009;**1**:323-37.
10. Martin SA, McCabe N, Mullarkey M, Cummins R, Burgess DJ, Nakabeppu Y, et al. DNA polymerases as potential therapeutic targets for cancers deficient in the DNA mismatch repair proteins MSH2 or MLH1. *Cancer Cell* 2010;**17**:235-48.
11. Farmer H, McCabe N, Lord CJ, Tutt AN, Johnson DA, Richardson TB, et al. Targeting the DNA repair defect in BRCA mutant cells as a therapeutic strategy. *Nature* 2005;**434**:917-21.
12. Bryant HE, Schultz N, Thomas HD, Parker KM, Flower D, Lopez E, et al. Specific killing of BRCA2-deficient tumours with inhibitors of poly(ADP-ribose) polymerase. *Nature* 2005;**434**:913-7.
13. Fong PC, Boss DS, Yap TA, Tutt A, Wu P, Mergui-Roelvink M, et al. Inhibition of poly(ADP-ribose) polymerase in tumors from BRCA mutation carriers. *N Engl J Med* 2009;**361**:123-34.
14. Hewish M, Martin SA, Elliott R, Cunningham D, Lord CJ, Ashworth A. Cytosine-based nucleoside analogs are selectively lethal to DNA mismatch repair-deficient tumour cells by enhancing levels of intracellular oxidative stress. *Br J Cancer* 2013;**108**:983-92.
15. Martin SA, Hewish M, Sims D, Lord CJ, Ashworth A. Parallel high-throughput RNA interference screens identify PINK1 as a potential therapeutic target for the

treatment of DNA mismatch repair-deficient cancers. *Cancer Res* 2011;**71**:1836-48.
16. Yip S, Miao J, Cahill DP, Iafrate AJ, Aldape K, Nutt CL, et al. Erratum: MSH6 mutations arise in glioblastomas during temozolomide therapy and mediate temozolomide resistance. *Clin Cancer Res* 2013;**19**:4543-4.
17. Busch AE, Suessbrich H, Kunzelmann K, Hipper A, Greger R, Waldegger S, et al. Blockade of epithelial Na+ channels by triamterenes - underlying mechanisms and molecular basis. *Pflugers Arch* 1996;**432**:760-6.
18. Zimmerman J, Selhub J, Rosenberg IH. Competitive inhibition of folic acid absorption in rat jejunum by triamterene. *J Lab Clin Med* 1986;**108**:272-6.
19. Ho PI, Ashline D, Dhitavat S, Ortiz D, Collins SC, Shea TB, et al. Folate deprivation induces neurodegeneration: roles of oxidative stress and increased homocysteine. *Neurobiol Dis* 2003;**14**:32-42.
20. Tung CL, Chiu HC, Jian YJ, Jian YT, Chen CY, Syu JJ, et al. Down-regulation of MSH2 expression by an Hsp90 inhibitor enhances pemetrexed-induced cytotoxicity in human non-small-cell lung cancer cells. *Exp Cell Res* 2014;**322**:345-54.
21. Le DT, Uram JN, Wang H, Bartlett BR, Kemberling H, Eyring AD, et al. PD-1 Blockade in Tumors with Mismatch-Repair Deficiency. *N Engl J Med* 2015;**372**:2509-20.

FIGURE LEGENDS

FIGURE 1. Triamterene sensitizes MMR-deficient cells

(**A**) Western blot analysis of protein lysates from DLD1 and DLD1+Chr2 cells. Protein expression was measured using MSH6 and β-actin antibodies. β-actin was used as a loading control.

(**B**) Western blot analysis of protein lysates from U251 and U251.TR3 cells. Protein expression was measured using MSH6 and β-actin antibodies. β-actin was used as a loading control.

(**C**) Western blot analysis of protein lysates from a panel of MMR-proficient (KLE, MFE-280) and MMR-deficient (AN3CA, MFE-296, ISHIKAWA, HEC1B, HEC59, RL95-2) endometrial cancer cell lines. Protein expression was measured using indicated antibodies. β-tubulin was used as a loading control.

(**D**) MSH6-proficient DLD1+Chr2 and MSH6-deficient DLD1 colorectal cell lines were treated with increasing concentrations of Triamterene (0, 2 μM, 4 μM, 6 μM, 8 μM & 10 μM). After 4 days treatment, cell viability was measured using an ATP-based luminescence assay.

(**E**) MSH6-proficient U251 and MSH6-deficient U251.TR3 cells were treated with increasing concentrations of Triamterene (0, 5 μM, 10 μM, 15 μM & 20 μM). After 4 days treatment, cell viability was measured using an ATP-based luminescence assay.

(**F**) A panel of MMR-proficient (KLE, MFE-280) and MMR-deficient (AN3CA, MFE-296, ISHIKAWA, HEC1B, HEC59, RL95-2,) endometrial cancer cell lines were treated with increasing concentrations of Triamterene (0, 10 μM, 20 μM, 30 μM & 40 μM). After 4 days treatment, cell viability was measured using an ATP-based luminescence assay.

(**G**) MSH6-proficient DLD1+Chr2 and MSH6-deficient DLD1 colorectal cell lines were treated with Triamterene (0, 8 μM & 10 μM). After 10-14 days treatment, cell survival was measured by counting sulphorhodamine‑B stained colonies.

(**H**) MLH1-proficient HCT116+Chr3 and MLH1-deficient HCT116 colorectal cancer cell lines were treated with increasing concentrations of Triamterene (0, 2 μM, 4 μM, 6 μM, 8 μM & 10 μM). After 4 days treatment, cell viability was measured using an ATP-based luminescence assay.

D-H: Data represent mean ± SEM of three independent experiments.

FIGURE 2. Triamterene is selective via its anti-folate activity and requires thymidylate synthase expression

(**A**) MSH6-proficient U251 and MSH6-deficient U251.TR3 GBM cells were transfected with either control non-targeting siRNA (siCTRL) or siRNA targeting the different isoforms of the epithelial sodium channel, ENaC (α, β & γ), either alone or in combination. 4 days post transfection, cell viability was measured using an ATP-based luminescence assay.

(**B**) U251 and U251.TR3 GBM cells were treated with either Control (DMSO; 0.01%), Triamterene (20 μM), Dihydrofolate (DHF; 10 μM), Tetrahydrofolate (THF; 10 μM) alone or combinations of DHF (10 μM) or THF (10 μM) with Triamterene (20 μM). After 4 days treatment, cell viability was measured using an ATP-based luminescence assay. **p<0.0001

(**C**) DLD1 and DLD1+Chr2 cells were treated with either media or Triamterene (10 μM), alone or in combination with dihydrofolate (DHF; 10 μM) or tetrahydrofolate (THF; 10 μM). After 4 days treatment, cell viability was measured using an ATP-based luminescence assay. **p≤0.007.

(**D**) Western blot analysis of protein lysates from U251 and U251.TR3 cells treated with either DMSO (0.01%) or Triamterene (10 μM) for 48 hrs. Protein expression was analysed using anti-TS (thymidylate synthase) and β-actin antibodies. β-actin was used as a loading control.

(**E**) U251 and U251.TR3 cells were transfected with control non-targeting siRNA (siCTRL) or siRNA targeting thymidylate synthase (siTS*1, siTS*2). After 24 hrs, cells were treated with either DMSO (0.01%) or increasing concentrations of Triamterene (0, 4 μM, 8 μM, 12 μM, 16 μM & 20 μM). After 4 days treatment, cell viability was measured using an ATP-based luminescence assay. *p=0.0025, **p=0.0001.

(**F**) DLD1 and DLD1+Chr2 cells were transfected with either control non-targeting siRNA (siCTRL) or siRNA targeting thymidylate synthase (siTS*1, siTS*2). After 24 hrs, cells were treated with either DMSO (0.01%) or increasing concentrations of Triamterene (0, 2 μM, 4 μM, 6 μM, 8 μM & 10 μM). After 4 days treatment, cell viability was measured using an ATP-based luminescence assay. *p≤0.01.

A-C, E & F: Data represent mean ± SEM of three independent experiments.

FIGURE 3. Triamterene treatment induces ROS in MMR-deficient cells

(**A**) U251 and U251.TR3 GBM cells were treated with either Control (DMSO; 0.01%), 10 μM or 20 μM Triamterene. After 48 hrs treatment, ROS levels were measured by quantifying the conversion of DCFDA into DCF by fluorescence. Fluorescence data were normalized to cell viability. *p≤0.04

(**B**) DLD1 and DLD1+Chr2 cells were treated with either Control (DMSO; 0.01%), 5 μM or 10 μM Triamterene. After 48 hrs treatment, ROS levels were measured by quantifying the conversion of DCFDA into DCF by fluorescence. Fluorescence data were normalized to cell viability. ***p≤0.0006.

(**C**) DLD1 and DLD1+Chr2 cells were treated with either Control (DMSO; 0.01%), or increasing concentrations of Triamterene (0, 2 μM, 4 μM, 6 μM, 8 μM & 10 μM) alone or in combination with the ROS scavenger N-Acetyl cysteine (NAC; 1 mg/mL). After 4 days treatment, cell viability was measured using an ATP-based luminescence assay. *p=0.03, **p≤0.004.

(**D**) U251 and U251.TR3 cells were transfected with either control non-targeting siRNA (siCTRL) or siRNA targeting thymidylate synthase (siTS*1, siTS*2). After 24 h, cells were treated with either DMSO (0.01%) or Triamterene (20 μM). After 48 h treatment, ROS levels were measured by quantifying the conversion of DCFDA into DCF by fluorescence. Fluorescence data were normalized to cell viability. **p≤0.007.

(**E**) DLD1 and DLD1+Chr2 cells were transfected with either control, non-targeting siRNA (siCTRL) or siRNA targeting thymidylate synthase (siTS*1, siTS*2). After 24 hrs, cells were treated with either DMSO (0.01%) or Triamterene (10 μM). After 48 hrs treatment, ROS levels were measured by quantifying the conversion of DCFDA into DCF by fluorescence. Fluorescence data were normalized to cell viability. **p≤0.002.

A- E: Data represent mean ± SEM of three independent experiments.

FIGURE 4. Triamterene treatment induces cellular DNA damage and G2/M arrest in MMR-deficient cells

(**A**) DLD1 and DLD1+Chr2 cells were treated with either Control (DMSO; 0.01%), or Triamterene (10 μM). FACS analysis was performed 24 h after Triamterene treatment. Data was normalized to initial numbers of cells in the G2/M phase of the cell cycle. Assays were performed in triplicate and bar chart shows the fold change in cells in the G2/M phase of the cell cycle in each cell line. **p≤0.001.

(**B**) DLD1 and DLD1+Chr2 cells were treated with either Control (DMSO; 0.01%), or Triamterene (10 μM). After 48 h cells were mixed with molten agarose, DNA was

denatured and electrophoresed in a horizontal chamber. Stained DNA was visualized by fluorescence microscopy. Cellular DNA damage was visualised as a comet tail shape. Assays were performed in triplicate and bar chart shows the % of tail DNA observed in each cell line. ***p≤0.0001.

(**C**) DLD1 and DLD1+Chr2 cells were treated with either Control (DMSO; 0.01%), or Triamterene (10 μM). After 48 h, DNA was extracted and 8-oxodG was quantified according to a standard curve. Assays were performed in triplicate and bar chart shows the fold change in 8-oxodG lesions in each cell line. *p≤0.01.

(D) Schematic model of the sensitizing effect of Triamterene in MMR-deficient cells

FIGURE 5. Triamterene treatment induces DNA DSBs in MMR-deficient cells, which can be rescued by addition of N-Acetyl cysteine

(**A**) Representative images of γH2AX foci, quantified by confocal microscopy in U251 and U251.TR3 cells upon treatment with either PBS or NAC (10 mg/mL) alone or in combination with DMSO (0.01%) or Triamterene (20 μM). Nuclei are shown in blue (DAPI) and γH2AX foci are in red.

(**B**) DLD1 and DLD1+Chr2 cells were treated with either PBS or NAC (10 mg/mL) alone or in combination with DMSO (0.01%) or Triamterene (10 μM). After 48 hrs treatment, cells were fixed, stained using a γH2AX antibody and DAPI, and observed by confocal microscopy. Per condition, a minimum of 300 cells were counted and quantified for γH2AX positive cells (> 5 foci per nucleus). ***p≤0.0001.

(**C**) U251 and U251.TR3 cells were treated with either Control (DMSO; 0.01%), Triamterene (20 μM) or NAC (10 mg/mL) alone or in combination. After 24 hrs treatment, cells were fixed, stained using a γH2AX antibody and DAPI and observed by confocal microscopy. Per condition, a minimum of 300 cells were counted and quantified for γH2AX positive cells (> 5 foci per nucleus). ***p≤0.0008.

(**D**) Representative images of γH2AX foci, quantified by confocal microscopy in DLD1 and DLD1+Chr2 cells upon treatment with either PBS or NAC (10 mg/mL) alone or in combination with DMSO (0.01%) or Triamterene (10 μM). Nuclei are shown in blue (DAPI) and γH2AX foci are in red.

FIGURE 6. Triamterene sensitizes MMR-deficient cells, *in vivo*

In vivo efficacy experiments were performed on 20 NOD-SCID mice injected with either DLD1 cells (**A**; 1.6 x 10^6 cells) or DLD1+Chr2 cells (**B**; 1.6 x 10^6 cells). When the tumors

were measurable, mice were treated 3 times a week by gavage with 25 mg/kg Triamterene or vehicle. Tumors were measured twice a week and tumor size was normalized to initial treatment measurements. Data represent mean ± SEM. **p=0.01. NS denotes a p >0.05.

FIGURE 1

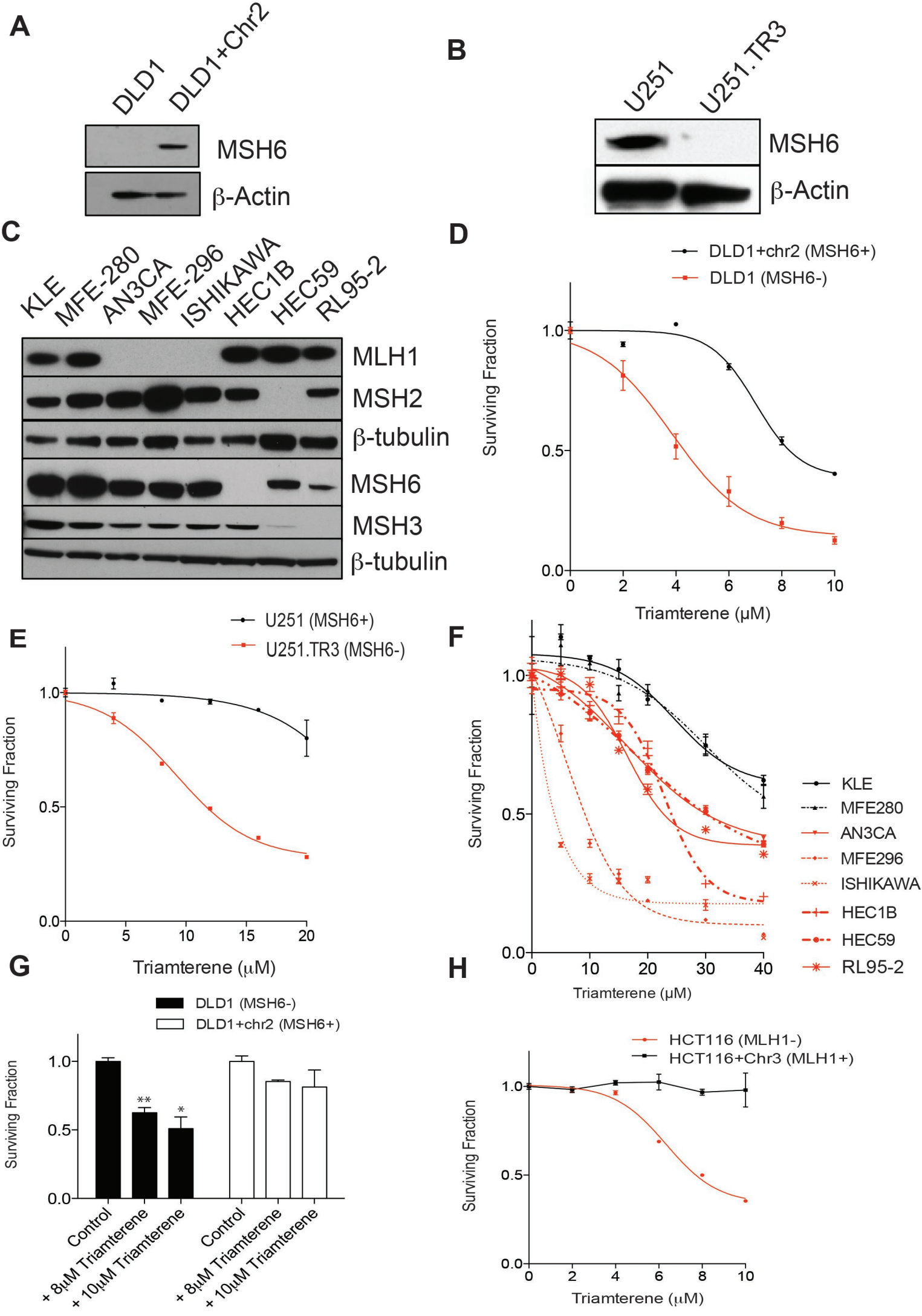
A
DLD1
DLD1+Chr2
MSH6
β-Actin
B
U251
U251.TR3
MSH6
β-Actin
C
KLE
MFE-280
AN3CA
MFE-296
ISHIKAWA
HEC1B
HEC59
RL95-2
MLH1
MSH2
β-tubulin
MSH6
MSH3
β-tubulin
D
DLD1+chr2 (MSH6+)
DLD1 (MSH6-)
Surviving Fraction
Triamterene (μM)
E
U251 (MSH6+)
U251.TR3 (MSH6-)
Surviving Fraction
Triamterene (μM)
F
Surviving Fraction
Triamterene (μM)
KLE
MFE280
AN3CA
MFE296
ISHIKAWA
HEC1B
HEC59
RL95-2
G
DLD1 (MSH6-)
DLD1+chr2 (MSH6+)
Surviving Fraction
Control
+ 8μM Triamterene
+ 10μM Triamterene
H
HCT116 (MLH1-)
HCT116+Chr3 (MLH1+)
Surviving Fraction
Triamterene (μM)

FIGURE 2

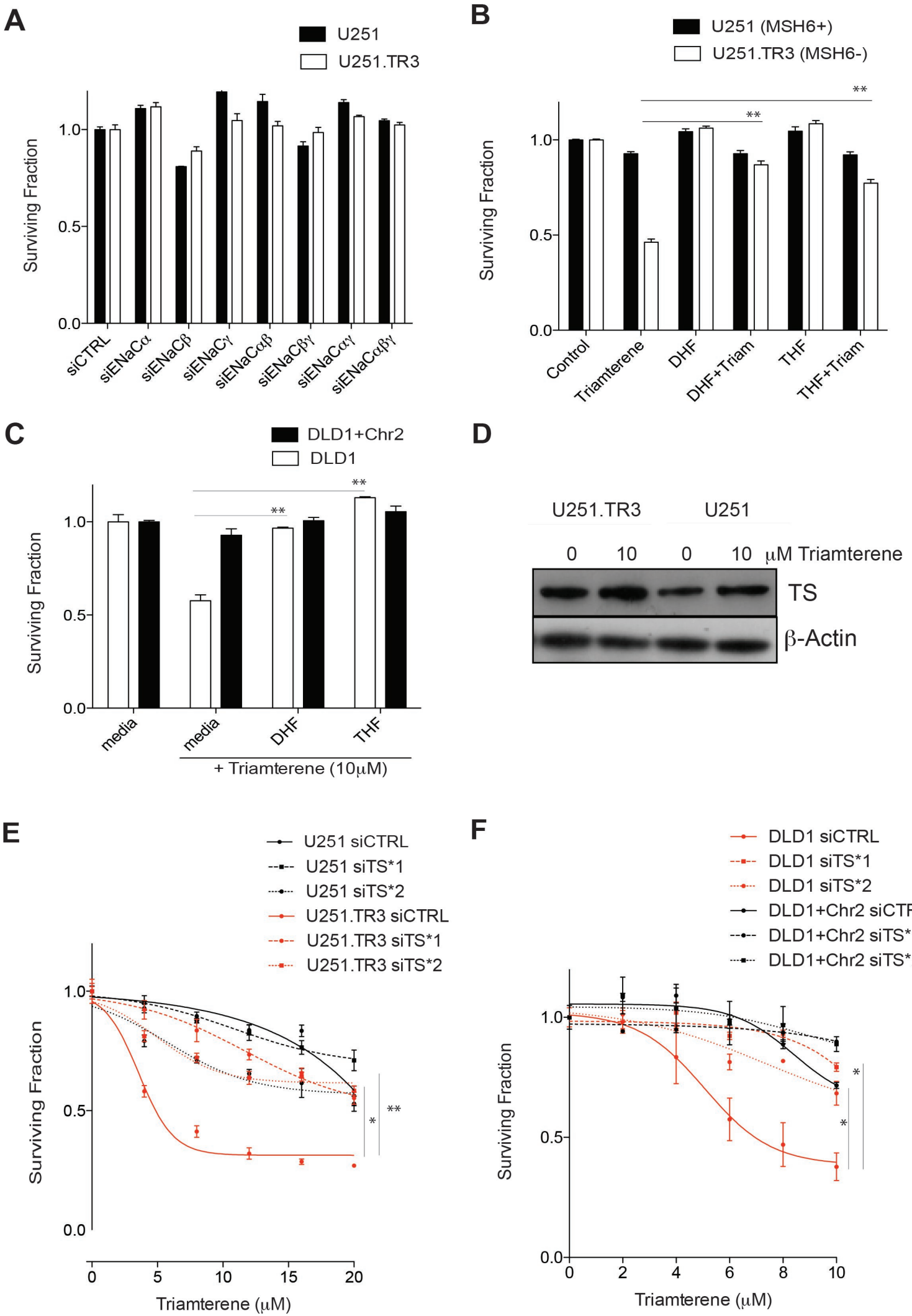
A
U251
U251.TR3
Surviving Fraction
1.0
0.5
0.0
siCTRL
siENaCα
siENaCβ
siENaCγ
siENaCαβ
siENaCβγ
siENaCαγ
siENaCαβγ
B
U251 (MSH6+)
U251.TR3 (MSH6-)
**
**
Surviving Fraction
1.0
0.5
0.0
Control
Triamterene
DHF
DHF+Triam
THF
THF+Triam
C
DLD1+Chr2
DLD1
**
**
Surviving Fraction
1.0
0.5
0.0
media
media
DHF
THF
+ Triamterene (10μM)
D
U251.TR3
U251
0
10
0
10
μM Triamterene
TS
β-Actin
E
U251 siCTRL
U251 siTS*1
U251 siTS*2
U251.TR3 siCTRL
U251.TR3 siTS*1
U251.TR3 siTS*2
Surviving Fraction
1.0
0.5
0.0
*
**
0
5
10
15
20
Triamterene (μM)
F
DLD1 siCTRL
DLD1 siTS*1
DLD1 siTS*2
DLD1+Chr2 siCTRL
DLD1+Chr2 siTS*1
DLD1+Chr2 siTS*2
Surviving Fraction
1.0
0.5
0.0
*
*
0
2
4
6
8
10
Triamterene (μM)

FIGURE 3

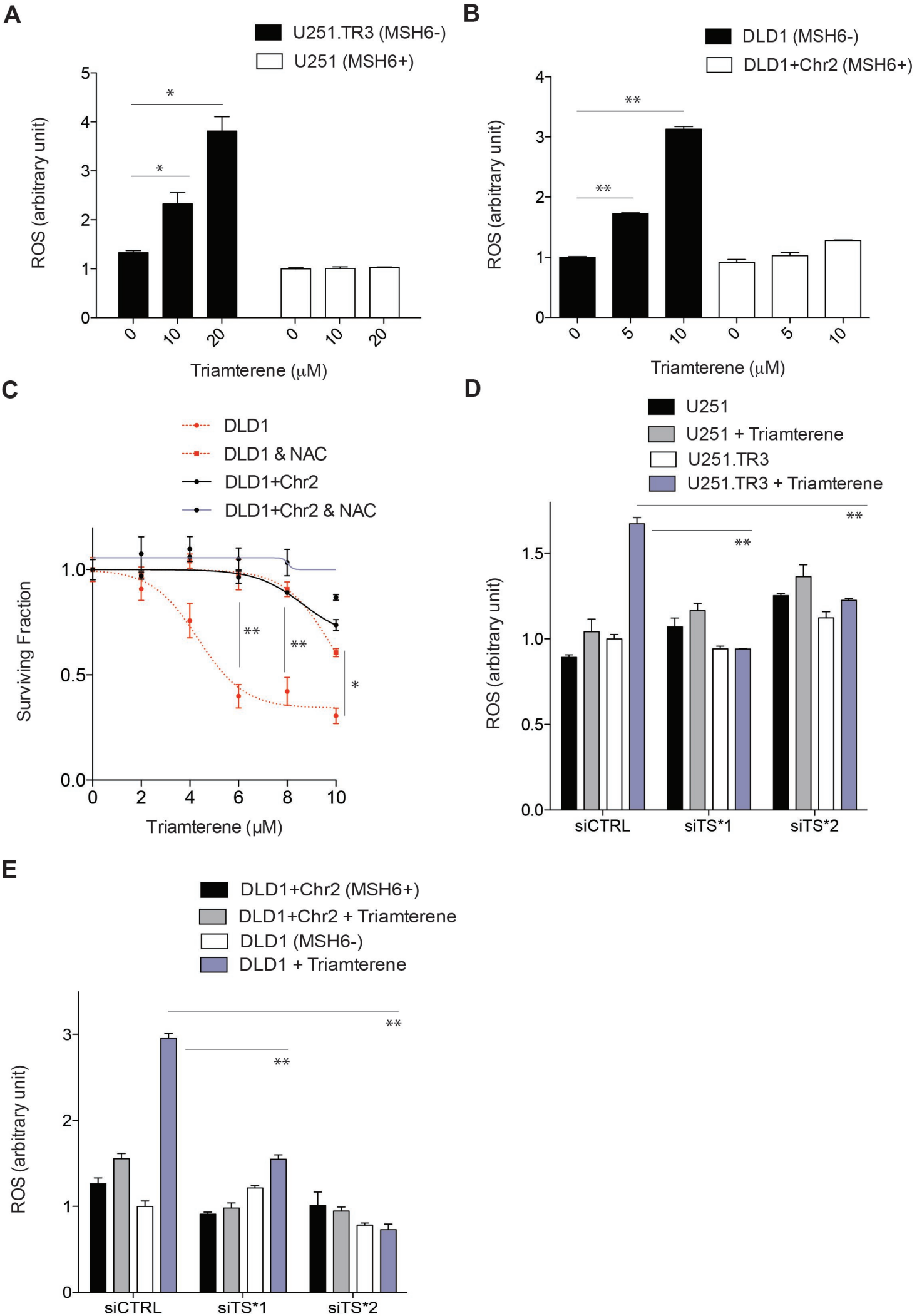
A
U251.TR3 (MSH6-)
U251 (MSH6+)
ROS (arbitrary unit)
Triamterene (μM)
B
DLD1 (MSH6-)
DLD1+Chr2 (MSH6+)
ROS (arbitrary unit)
Triamterene (μM)
C
DLD1
DLD1 & NAC
DLD1+Chr2
DLD1+Chr2 & NAC
Surviving Fraction
Triamterene (μM)
D
U251
U251 + Triamterene
U251.TR3
U251.TR3 + Triamterene
ROS (arbitrary unit)
siCTRL
siTS*1
siTS*2
E
DLD1+Chr2 (MSH6+)
DLD1+Chr2 + Triamterene
DLD1 (MSH6-)
DLD1 + Triamterene
ROS (arbitrary unit)
siCTRL
siTS*1
siTS*2

FIGURE 4

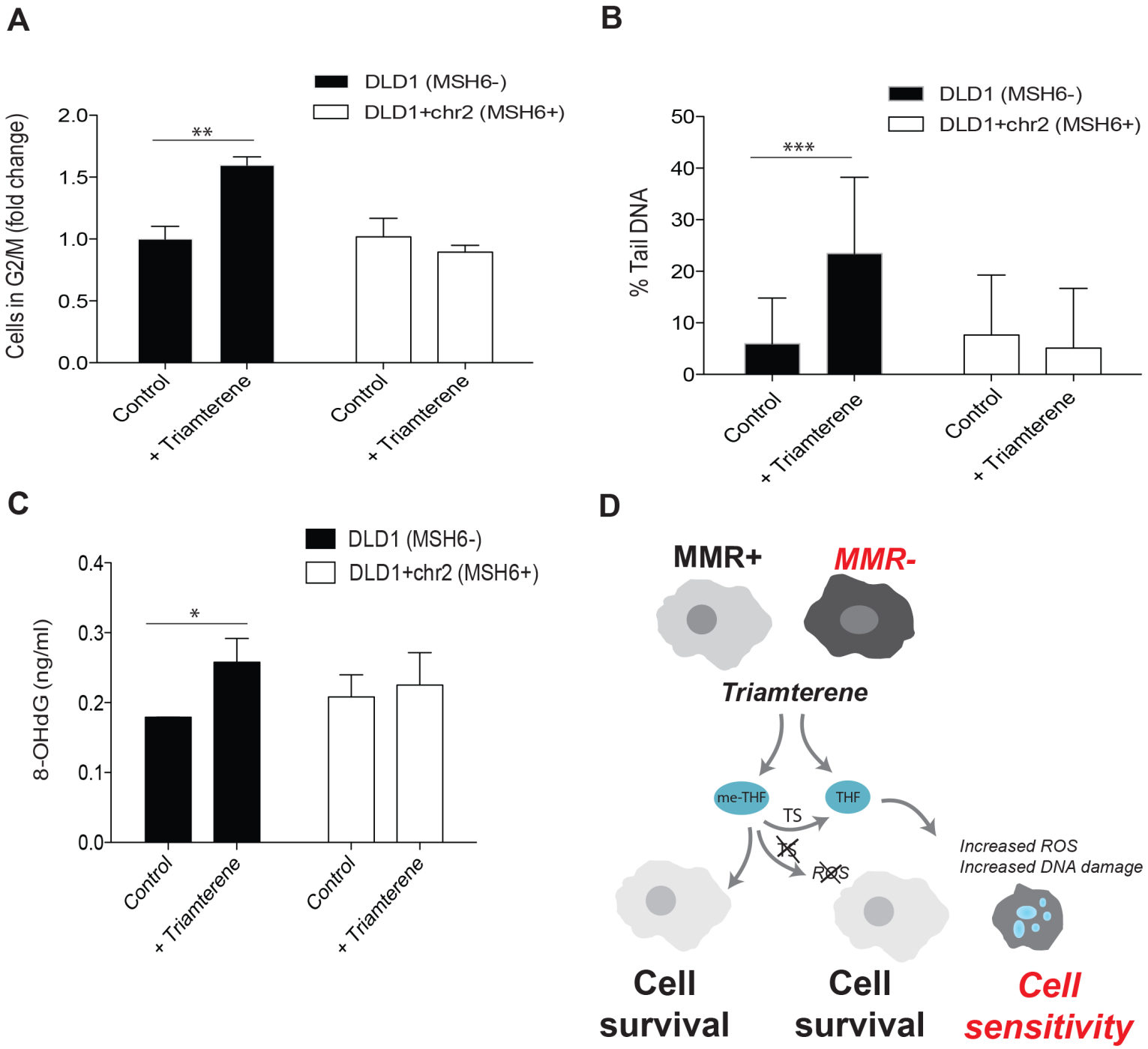
A
DLD1 (MSH6-)
DLD1+chr2 (MSH6+)
Cells in G2/M (fold change)
2.0
1.5
1.0
0.5
0.0
**
Control
+ Triamterene
Control
+ Triamterene
B
DLD1 (MSH6-)
DLD1+chr2 (MSH6+)
% Tail DNA
50
40
30
20
10
0
***
Control
+ Triamterene
Control
+ Triamterene
C
DLD1 (MSH6-)
DLD1+chr2 (MSH6+)
8-OHdG (ng/ml)
0.4
0.3
0.2
0.1
0.0
*
Control
+ Triamterene
Control
+ Triamterene
D
MMR+
MMR-
Triamterene
me-THF
THF
TS
TS
ROS
Increased ROS
Increased DNA damage
Cell survival
Cell survival
Cell sensitivity

FIGURE 5

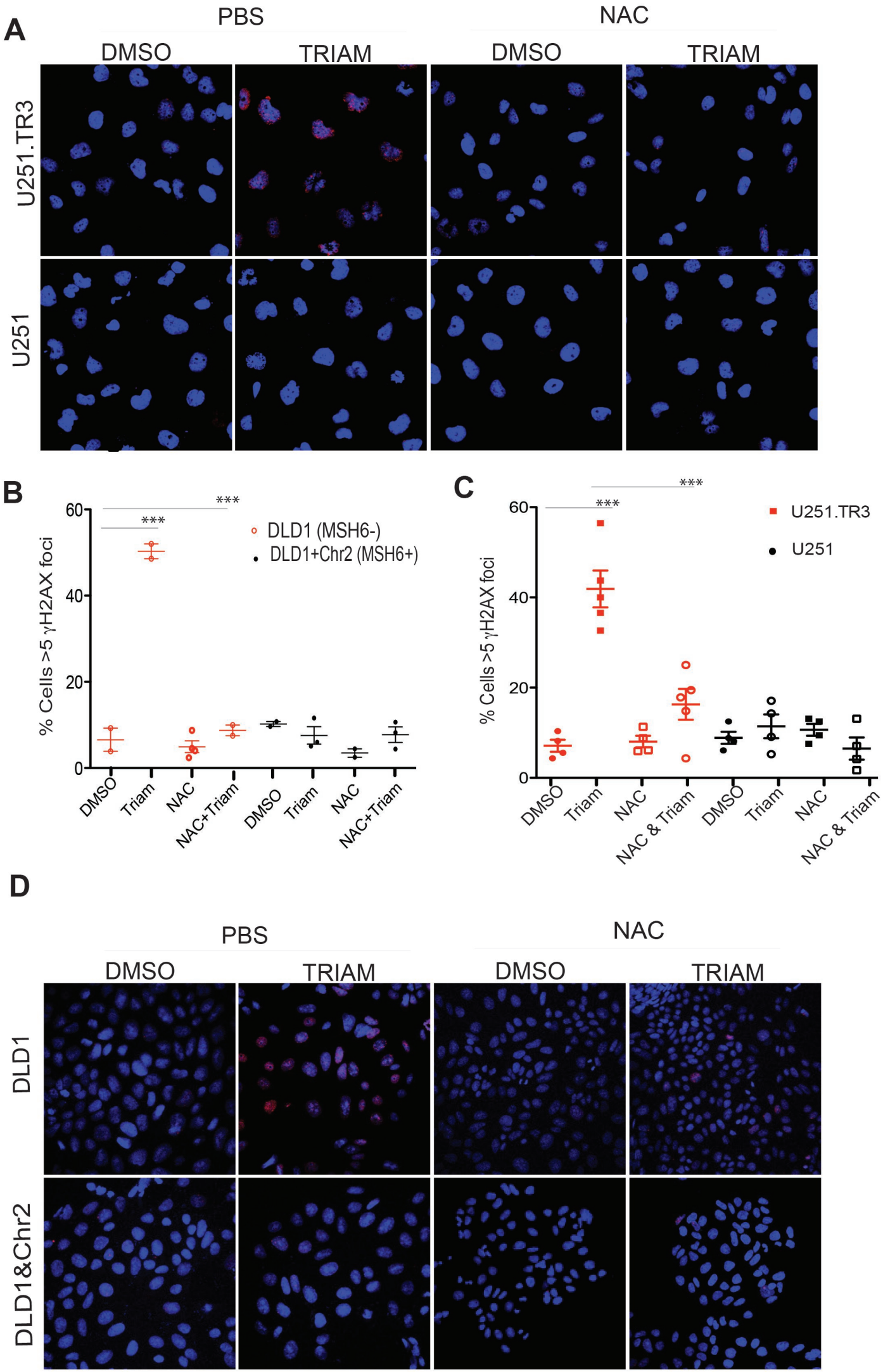
A
PBS
NAC
DMSO
TRIAM
DMSO
TRIAM
U251.TR3
U251
B
% Cells >5 γH2AX foci
60
40
20
0
***
***
DLD1 (MSH6-)
DLD1+Chr2 (MSH6+)
DMSO
Triam
NAC
NAC+Triam
DMSO
Triam
NAC
NAC+Triam
C
% Cells >5 γH2AX foci
60
40
20
0
***
***
U251.TR3
U251
DMSO
Triam
NAC
NAC & Triam
DMSO
Triam
NAC
NAC & Triam
D
PBS
NAC
DMSO
TRIAM
DMSO
TRIAM
DLD1
DLD1&Chr2

FIGURE 6

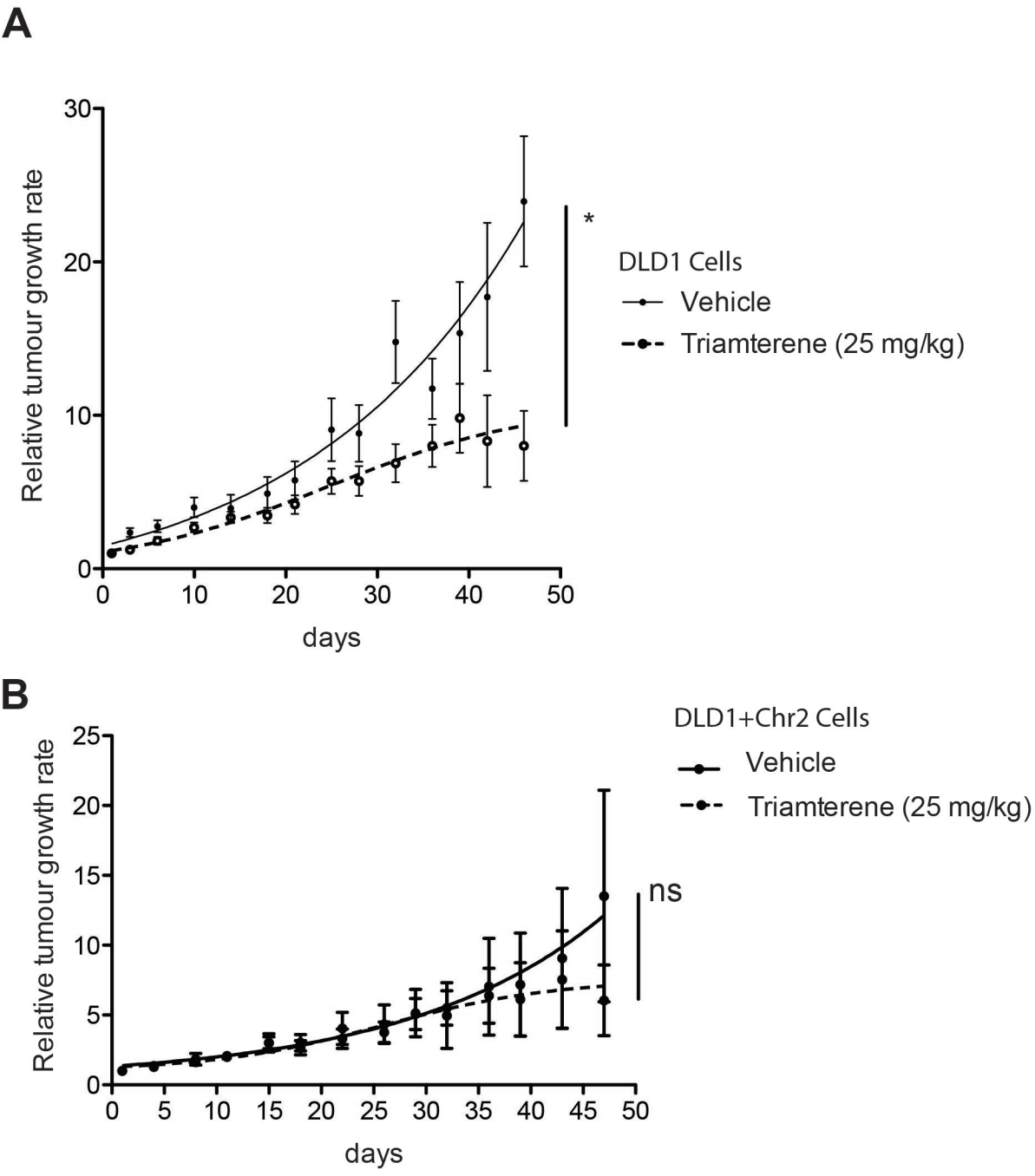
A
Relative tumour growth rate
30
20
10
0
0
10
20
30
40
50
days
*
DLD1 Cells
Vehicle
Triamterene (25 mg/kg)
B
Relative tumour growth rate
25
20
15
10
5
0
0
5
10
15
20
25
30
35
40
45
50
days
ns
DLD1+Chr2 Cells
Vehicle
Triamterene (25 mg/kg)